The original version published January 31, 2007, contained errors.
The corrected version was published August 29, 2007.

Supporting Information

Conjugation-Length Dependence of the T_1 Lifetimes of Carotenoids Free in Solution and Incorporated into the LH2, LH1, RC and RC-LH1 Complexes: Possible Mechanisms of Triplet-Energy Dissipation

Yoshinori Kakitani[‡], Junji Akahane[‡], Hidekazu Ishii[‡], Hiroshi Sogabe[‡], Hiroyoshi Nagae,[§] and Yasushi Koyama[*,‡]

[‡] *Faculty of Science and Technology, Kwansei Gakuin University, Gakuen, Sanda 669-1337, Japan, and* [§] *Kobe City University of Foreign Studies, Gakuen-Higashimachi, Nishi-ku, Kobe 651-2187, Japan*

Sample Preparations: (a) The Isolation of Methoxyneurosporene and Tetrahydrospirilloxanthin. The Car pigments extracted from *Rba. sphaeroides* Ga with acetone was subjected to funnel separation between petroleum-ether and saturated NaCl aqueous solution; the lipid component was carefully removed. After drying with anhydrous Na_2SO_4, the organic phase was dried *in vacuo*, and the residue was dissolved into *n*-hexane. The solution was subjected to repeated column chromatography using alumina (Alminum oxide 90 standardized; Merck KGaA, Germany). The column was developed with an eluent consisting of diethyl ether in *n*-hexane; methoxyneurosporene and tetrahydrospirilloxanthin eluted at 7% and 15% diethyl ether in *n*-hexane, respectively. For complete removal of lycopene from methoxyneurosporene, low-pressure column chromatography (Yamazen Corp., Japan), using calcium hydroxide (lot. E48215T; Kishida Chemical Co., Ltd., Japan) as the packing material and 10–20% acetone in benzene as an eluent, was applied (*S1*).

(b) The Isolation of the RCs from Rba. sphaeroides G1C and 2.4.1. Choromatophores in 20 mM Tris-HCl buffer (pH 8.0; OD_{850} = 50 cm^{-1}) was first solubilized with 0.15% *N*,*N*-dimethyldodecylamine-*N*-oxide (LDAO; Fluka Chemie GmbH, Germany) at 27–28 ºC for 30 min, and then, centrifuged (278,000*g*, 4 ºC, 1 h) to remove the LH2 complex. The residual was resuspended (OD_{850} = 50 cm^{-1}) in the same buffer containing 150 mM NaCl, and solubilized again under the same conditions. After dialysis against 0.1% LDAO in 20 mM Tris-HCl (pH 8.0), the supernatant (crude RC) was subjected to DE52 ion-exchange column chromatography (Whatman International Ltd., United Kingdom). A fraction showing $OD_{280}/OD_{800} < 1.4$ was collected in each RC preparation.

(c) The Isolation of the RC from Rsp. rubrum S1. Chromatophores suspended in a 50 mM potassium phosphate buffer (pH 7.5; OD_{880} = 100 cm^{-1}) was first solubilized with 0.30% LDAO at 0 ºC for 1 h, a 3 equiv volume of 50 mM potassium phosphate buffer (pH 7.5) was added to stop the solubilization, and centrifuged (278,000*g*, 4 ºC, 1 h). The residual was resuspended in the same buffer (OD_{880} = 100 cm^{-1}) and solubilized again under the same conditions (this solubilization procedure was repeated twice). The RC thus obtained was purified by ultrafiltration (UHP-43K; Toyo Roshi, Ltd., Japan) using a membrane filter (MWCO 50,000; Toyo Roshi, Ltd., Japan).

Ground-State Electronic Absorption Spectra of the LH1, RC, and RC-LH1 Complexes.

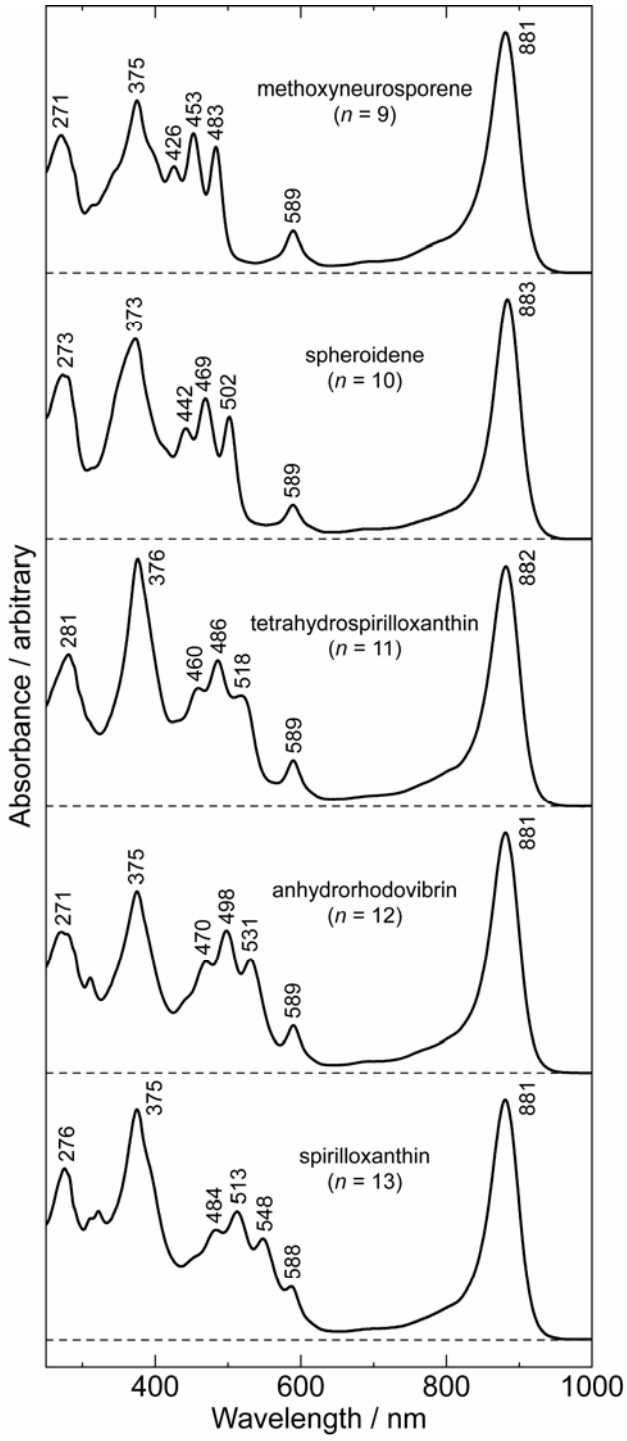

FIGURE S1: Ground-state absorption spectra of the LH1 complexes from *Rsp. rubrum* G9 to which methoxyneurosporene ($n = 9$), spheroidene ($n = 10$), tetrahydrospirilloxanthin ($n = 11$), anhydrorhodovibrin ($n = 12$), and spirilloxanthin ($n = 13$) were incorporated ('the reconstituted LH1 complexes').

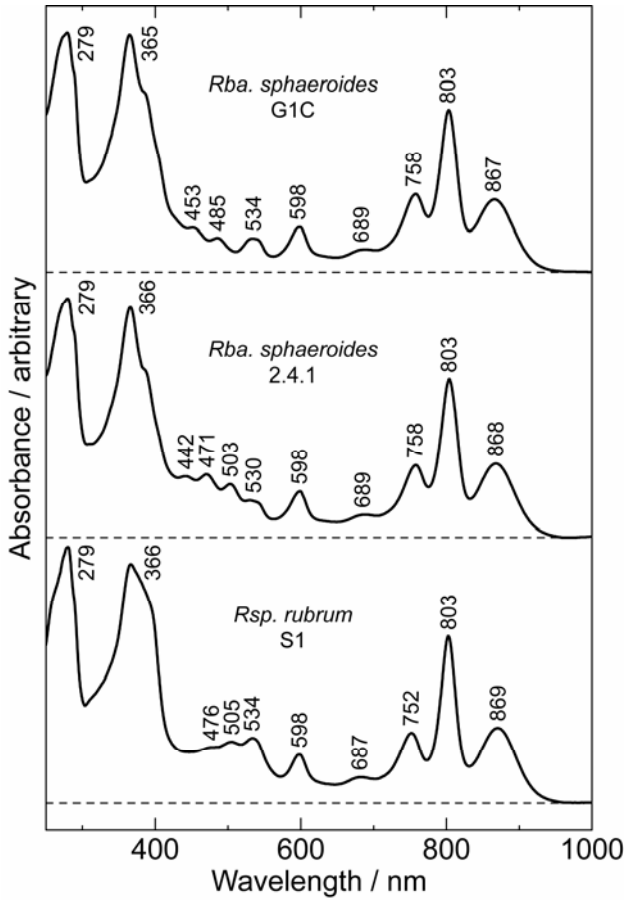

FIGURE S2: Ground-state absorption spectra of the RCs from *Rba. sphaeroides* G1C, *Rba. sphaeroides* 2.4.1, and *Rsp. rubrum* S1, containing major Cars with $n = 9$, 10, and 13, respectively (see Table 1b for the Car composition).

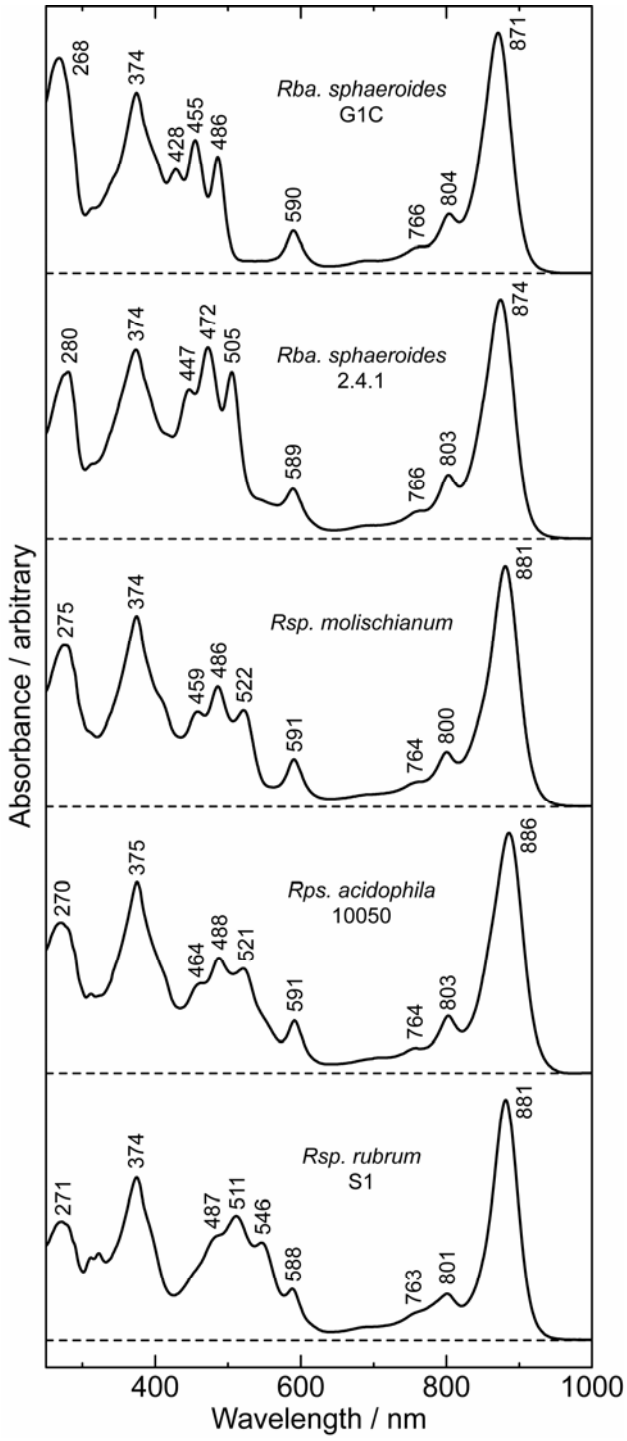

FIGURE S3: Ground-state absorption spectra of RC-LH1 complexes from *Rba. sphaeroides* G1C, *Rba. sphaeroides* 2.4.1, *Rsp. molischianum*, and *Rsp. rubrum* S1, containing major Cars, neurosporene (n = 9), spheroidene (n = 10), lycopene + rhodopin (n = 11), and spirilloxanthin (n = 13), respectively; that from *Rps. acidophila* 10050 containing multiple Cars, lycopene (n = 11), rhodopin glucoside (n = 11), anhydrorhodovibrin (n = 12), and spirilloxanthin (n = 13) is also shown (see Table 1c for the Car compositions).

Enhanced Intersystem Crossing due to the Twisting of the Conjugated Chain in the LH2-Bound All-trans-Rhodopin Glucoside and the RC-Bound 15-cis-Spheroidene. In the adiabatic approximation, or in other words, the Born Oppenheimer (BO) approximation, the state of a molecular system can be described by the product of wavefunctions,

$$\Psi_{nv} = \psi_n \chi_{nv}, \tag{1'}$$

where ψ_n is the wavefunction for the electrons of the system, in which the nuclei is supposed to be fixed at their instantaneous positions, and χ_{nv} designates the wavefunction of intramolecular vibrations of the system. These wavefunctions, ψ_n and χ_{nv}, are the solutions of the following coupled Schrödinger equations:

$$[T_e + V_e(Q)]\psi_n(Q) = E_n(Q)\psi_n(Q) \tag{2'}$$

$$[T_Q + E_n(Q)]\chi_{nv}(Q) = W_{nv}\chi_{nv}(Q) \tag{3'}$$

with

$$V_e(Q) = \sum_{i>j=1}^{n_{elec}} \frac{e^2}{\left|\vec{r}_i - \vec{r}_j\right|} - \sum_{i=1}^{n_{elec}} \sum_{r=1}^{n_{nucl}} \frac{z_r e^2}{\left|\vec{r}_i - \vec{R}_r\right|} + \sum_{r>s=1}^{n_{nucl}} \frac{z_r z_s e^2}{\left|\vec{R}_r - \vec{R}_s\right|}, \tag{4'}$$

where T_e (T_Q) stands for the kinetic energy of the electrons (nuclei), $\vec{r}_i$ ($\vec{R}_r$) represents the positional vector of the *i*-th electron (*r*-th nucleus), $z_r e$ is the charge on the *r*-th nucleus, $Q = \{Q_j\}$ are the set of nuclear normal coordinates, *v* signifies the vibrational states of the nuclei, and Eq. (2') contains the nuclear coordinate, *Q*, as a parameter.

In the intersystem crossing process between states, in the BO approximation, the perturbation which causes the transition is the spin-orbit coupling,

$$H_{SO}(Q) = \sum_{i=1}^{n_{elec}} \sum_{r=1}^{n_{nucl}} \varsigma_r(\left|\vec{r}_i - \vec{R}_r\right|)\vec{l}_{ri} \cdot \vec{s}_i, \tag{5'}$$

where $\vec{l}_{ri}$ is the angular momentum of the *i*-th electron around the *r*-th nucleus, $\vec{s}_i$ is the spin-angular momentum of the *i*-th electron, and $\varsigma_r\left(\left|\vec{r}_i - \vec{R}_r\right|\right)$ accounts for the interaction of the electron with a field produced by the nucleus. According to the standard time-dependent perturbation theory, the rate of

intersystem crossing from the *n*-th to the *m*-th electronic state can be expressed as

$$k = \frac{2\pi}{\hbar} \sum_u \sum_v B_u \left| C \right|^2 \delta \left(\Delta E + E_v - E_u \right) \tag{6'}$$

with

$$C = \left\langle \chi_{mv}(Q) \psi_m(Q) \left| H_{SO}(Q) \right| \psi_n(Q) \chi_{nv}(Q) \right\rangle, \tag{7'}$$

where B_u is the Boltzmann factor, ΔE is the electronic-energy difference between the initial and final states, E_u and E_v are the vibrational energies of the initial and final states, respectively. Defining $H_{SO}^{mn}(Q)$ as

$$H_{SO}^{mn}(Q) = \left\langle \psi_m(Q) \left| H_{SO}(Q) \right| \psi_n(Q) \right\rangle_{el}, \tag{8'}$$

Eq. (7') can be expressed as

$$C = \left\langle \chi_{mv}(Q) \left| H_{SO}^{mn}(Q_0) \right| \chi_{nu}(Q) \right\rangle + \left\langle \chi_{mv}(Q) \left| \sum_j \left(\frac{\partial H_{SO}^{mn}(Q)}{Q_j} \right)_0 Q_j \right| \chi_{nu}(Q) \right\rangle. \tag{9'}$$

In the following, we will use the dimensionless normal coordinates defined by

$$q_j = \sqrt{\frac{\omega_j}{\hbar}} Q_j, \tag{10'}$$

where ω_j is the angular frequency of the *j*-th normal mode in the initial state *n*. Considering that the phases of normal coordinates (q_j) are independent from each other, and the cross term, $q_j q_k$ ($j \neq k$), vanishes on a statistical average, we have

$$\left| C \right|^2 = \left| H_{SO}^{mn}(q_0) \left\langle \chi_{mv}(q) \left| \chi_{nu}(q) \right\rangle \right|^2 + \sum_j \left| \left(\frac{\partial H_{SO}^{mn}(q)}{q_j} \right)_0 \left\langle \chi_{mv}(q) \left| q_j \right| \chi_{nu}(q) \right\rangle \right|^2. \tag{11'}$$

Inserting this equation into Eq. (6') leads to

$$k = \frac{2\pi}{\hbar} J^2 \sum_u \sum_v B_u \left| \left\langle \chi_{mv}(q) \left| \chi_{nu}(q) \right\rangle \right|^2 \delta \left(\Delta E + E_v - E_u \right) \tag{12'}$$

with

$$J^2 = \left| H_{SO}^{mn}(q_0) \right|^2 + \sum_j \left| \left(\frac{\partial H_{SO}^{mn}(q)}{q_j} \right)_0 \right|^2, \tag{13'}$$

where $\left\langle \chi_{mv}(q)\middle|q_j\middle|\chi_{nu}(q)\right\rangle$ is approximated by $\left\langle \chi_{mv}(q)\middle|\chi_{nu}(q)\right\rangle$. The intersystem crossing due to the first term of Eq. (13') is usually called 'the direct spin-orbit coupling' and that due to the second term, 'the vibronically induced spin-orbit coupling'.

In the case when one accepting mode is predominant, the rate can be approximated, in the high-temperature limit, by the Englman–Jortner equation (*S2*),

$$k = \frac{2\pi}{\hbar} J^2 \frac{1}{\sqrt{2\pi(\Delta E)\hbar\omega}} \exp\left(-\frac{1}{2}\Delta^2\right) \exp\left[-\frac{\gamma(\Delta E)}{\hbar\omega}\right] \tag{14'}$$

with

$$\gamma = \ln\frac{2(\Delta E)}{\Delta^2\hbar\omega} - 1, \tag{15'}$$

where ω and Δ are the angular frequency and the shift of the potential minimum, concerning the dominant accepting mode, in the dimensionless normal coordinate.

In the following, we will calculate the rate of the T_1 to S_0 intersystem crossing of carotenoids due to the direct spin-orbit coupling mechanism. Denoting the T_1 states as $^3\Phi_x$, $^3\Phi_y$, $^3\Phi_z$, and the S_0 state as $^1\Phi_0$, J in this equation can be expressed by

$$J = \sqrt{\frac{1}{3}\left(\left|\left\langle {}^1\Phi_0\middle|H_{SO}\middle|{}^3\Phi_x\right\rangle\right|^2 + \left|\left\langle {}^1\Phi_0\middle|H_{SO}\middle|{}^3\Phi_y\right\rangle\right|^2 + \left|\left\langle {}^1\Phi_0\middle|H_{SO}\middle|{}^3\Phi_z\right\rangle\right|^2\right)}. \tag{16'}$$

If we take the values of $\Delta = 1.5$, $\Delta E = 7000$ cm^{-1} and $\hbar\omega = 1500$ cm^{-1}, we have $\gamma = 0.423$ and a rough estimation for the intersystem-crossing rate as

$$k = 6.58 \times 10^6 \, J^2 \ (\text{sec}^{-1}), \tag{17'}$$

where J is expressed in cm^{-1}. By the use of the INDO/S method together with assuming that the T_1 state can be well-described by moving an electron in the highest occupied molecular orbital to the lowest unoccupied molecular orbital, we can estimate the value of J for rhodopin glucoside in LH2 to be 0.0716 cm^{-1} ($1/k = 29.6$ μs) and that for spheroidene in RC to be 0.1849 cm^{-1} ($1/k = 4.5$ μs). The dihedral (torsional) angles along the conjugated chain were calculated based on the coordinates, determined by X-ray crystallography, for the LH2-bound rhodopin glucoside (PDB entry 1NKZ, *S3*) and the RC-bound spheroidene (PDB entry 1YST, *S4*).

Suppression of the Linear Dependence in the Correlation in the LH1 and RC Components of the RC-LH1 Complex. (a) Change in the Linear Dependence in LH1 in Core: The Role of Minor-Component Car. The mechanism of shortening of the T_1 lifetime of the major-component Car (n = 9), keeping the T_1 lifetimes of Car (n = 11) and Car (n = 13) almost unchanged (see Figure 8b), is shown by Scheme A in Scheme 1. The simulation was performed as follows: Let $n_1(t)$ be the probability of finding one major-component Car (out of fifteen) in the T_1 state, and $n_2(t)$ be the probability of finding the minor-component Car in the T_1 state. For simplicity, we assume the initial probabilities, $n_1(0) = n_2(0) = 1$. The decay dynamics of the triplet-excited states can be described by a pair of differential equations,

$$\frac{dn_1(t)}{dt} = -k_1 n_1(t) - k_3 n_1(t)\big(1 - n_2(t)\big)$$
$$\frac{dn_2(t)}{dt} = -k_2 n_1(t) + k_3 n_1(t)\big(1 - n_2(t)\big), \qquad (18')$$

where k_1 and k_2 are the intrinsic rates for the major-component and the minor-component Cars, respectively, and k_3 is an average rate for the triplet-energy transfer from the former to the latter. The non-linear equations can be solved numerically. The results are shown in the 1st panel of Figure S4: Assuming the triplet-energy transfer time constant (8.5 μs, see Scheme A) from the major-component Car (abbreviated as 'major Car') to the minor-component Car ('minor Car'), the intrinsic lifetime of the former (7.6 μs) shortens to an apparent lifetime (5.30 μs), whereas the intrinsic lifetime of the latter (4.0 μs) lengthens to an apparent lifetime (5.35 μs).

(b) Change in the Linear Dependence in RC in Core: The Role of BChl Triplet Reservoir. The mechanism of shortening the T_1 lifetime of Car (n = 9) and lengthening the T_1 lifetime of Car (n = 13), keeping that of Car (n = 11) unchanged (Figure 8b), is depicted by Scheme B in Scheme 1. For Car (n = 9), the T_1 lifetime becomes shorter when a neighboring BChl assembly in the ground state, whose T_1-state energy is lower than that of Car (n = 9), functions as an energy sink. For Car (n = 13), the T_1 lifetime becomes apparently longer, if a neighboring BChl in the T_1 state, that is above the T_1-state energy of Car (n = 13), functions as an energy supplier.

The case of Car (n = 9) can be simulated, as shown on the right-hand-side of Scheme B (practically the same as Scheme A), by simply assuming a partition between the intrinsic decay of the

shorter-chain Car and the triplet-energy transfer to the reservoir (11.8 μs); the intrinsic lifetime of Car (6.3 μs) shortens to the apparent lifetime (4.1 μs); the result is depicted in the 2nd panel of Figure S4. The case of Car (n = 13) was simulated, as shown on the left-hand-side of Scheme B, by the use of the following rate equations:

Let $n_1(t)$ be the probability of finding the Car in the T_1 state, and $n_2(t)$ be the probability of finding the reservoir BChl in the T_1 state. The decay dynamics of the triplet excited states can be described by a pair of differential equations,

$$\frac{dn_1(t)}{dt} = -k_1 n_1(t) + k_2 n_2(t)$$
$$\frac{dn_2(t)}{dt} = -k_2 n_2(t)\,, \qquad (19')$$

where k_1 is the intrinsic decay rate for the Car, and k_2 is the rate of the triplet-energy transfer from the BChl reservoir. Assuming that $n_1(0) = n_2(0) = 1$, $n_1(t)$ can be given as

$$n_1(t) = \frac{k_1 - 2k_2}{k_1 - k_2}\exp(-k_1 t) + \frac{k_2}{k_1 - k_2}\exp(-k_2 t)\,. \qquad (20')$$

The results are shown in the 3rd panel of Figure S4. Due to the triplet-energy transfer from the BChl triplet reservoir (7.0 μs), the intrinsic lifetime of the Car (2.3 μs) lengthens to an apparent lifetime (4.0 μs).

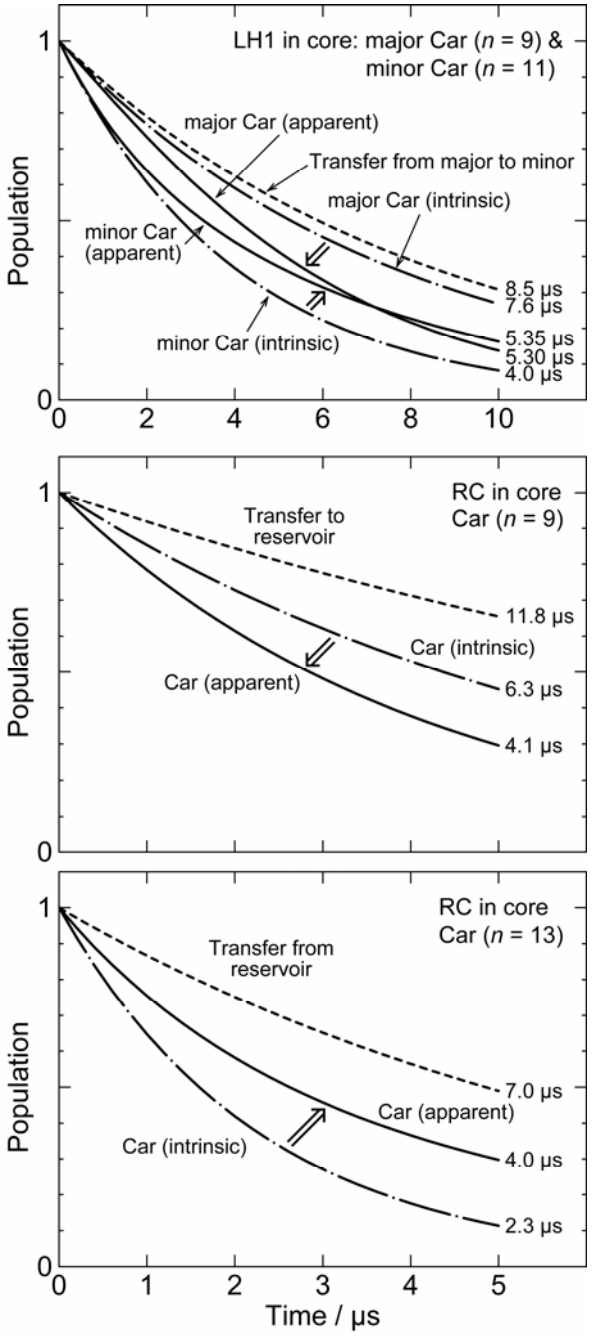

FIGURE S4: The decay time profiles simulated based on Scheme A and Scheme B in Scheme 1 by the use of the rate equations described in this subsection including (a) and (b). *LH1 in core* (top): The intrinsic decay profiles of major and minor Cars (dotted broken lines) shift to the apparent profiles (solid lines) downward and upward, respectively, when the triplet-energy transfer from the major to the minor component (broken line) introduced. *Car (n = 9) in RC in core* (middle): The intrinsic decay profile of Car ($n = 9$; dotted broken line) shift downward to the apparent profile (solid line), when the triplet-energy transfer from the Car to the BChl triplet-energy reservoir (broken line) is introduced. *Car (n = 13) in RC in core* (bottom): The intrinsic decay profile of Car ($n = 13$; dotted broken line) shift upward to the apparent profile (solid line), when the triplet-energy transfer from the BChl triplet-energy reservoir to the Car is introduced.

REFERENCES

S1. Furuichi, K., Sashima, T., and Koyama, Y. (2002) The first detection of the $3A_g^-$ state in carotenoids using resonance-Raman excitation profiles, *Chem. Phys. Lett. 356*, 547–555.

S2. Englman, R., and Jortner, J. (1970) The energy gap law for radiationless transitions in large molecules, *Mol. Phys. 18*, 145–164.

S3. Papiz, M. Z., Prince, S. M., Howard, T., Cogdell, R. J., Isaacs, N. W. (2003) The structure and thermal motion of the B800–850 LH2 complex from *Rps. acidophila* at 2.0 Å resolution and 100 K: New structural features and functionally relevant motions, *J. Mol. Biol. 326*, 1523–1538.

S4. Arnoux, B., Gaucher, J.-F., Ducruix, A., and Reiss-Husson, F. (1995) Structure of the photochemical reaction centre of a spheroidene-containing purple bacterium, *Rhodobacter sphaeroides* Y, at 3 Å resolution, *Acta Crystallogr. Sect. D 51*, 368–379.